UNCLASSIFIED

CENTRAL RESEARCH LIBRARY
DOCUMENT COLLECTION

OAK RIDGE NATIONAL LABORATORY LIBRARY
3 4456 0022209 7

ORNL-1997
Progress

cy. 5

INSTRUMENTATION AND CONTROLS DIVISION

SEMIANNUAL PROGRESS REPORT

FOR PERIOD ENDING JULY 31, 1955

CENTRAL RESEARCH LIBRARY
DOCUMENT COLLECTION

LIBRARY LOAN COPY

DO NOT TRANSFER TO ANOTHER PERSON

If you wish someone else to see this document, send in name with document and the library will arrange a loan.

OAK RIDGE NATIONAL LABORATORY
OPERATED BY
UNION CARBIDE NUCLEAR COMPANY
A Division of Union Carbide and Carbon Corporation
UCC
POST OFFICE BOX P · OAK RIDGE, TENNESSEE

UNCLASSIFIED

UNCLASSIFIED

ORNL-1997
Progress

COPY NO. 5

Contract No. W-7405-eng-26

INSTRUMENTATION AND CONTROLS DIVISION

SEMIANNUAL PROGRESS REPORT

For Period Ending July 31, 1955

C. J. Borkowski, Director

DATE ISSUED

DEC 13 1955

OAK RIDGE NATIONAL LABORATORY
Operated by
UNION CARBIDE NUCLEAR COMPANY
A Division of Union Carbide and Carbon Corporation
Post Office Box P
Oak Ridge, Tennessee

UNCLASSIFIED

OAK RIDGE NATIONAL LABORATORY
3 4456 0022209 7

ORNL-1997
Progress

INTERNAL DISTRIBUTION

1. C. E. Center
2. Biology Library
3. Health Physics Library
4-6. Central Research Library
7. Reactor Experimental Engineering Library
8-19. Laboratory Records Department
20. Laboratory Records, ORNL R.C.
21. A. M. Weinberg
22. S. J. Cromer
23. L. B. Emlet (K-25)
24. J. P. Murray (Y-12)
25. J. A. Swartout
26. E. H. Taylor
27. E. J. Murphy
28. E. D. Shipley
29. C. S. Harrill
30. F. C. VonderLage
31. W. H. Jordan
32. S. C. Lind
33. F. L. Culler
34. A. H. Snell
35. A. Hollaender
36. M. T. Kelley
37. K. Z. Morgan
38. T. A. Lincoln
39. A. S. Householder
40. C. E. Winters
41. D. W. Cardwell
42. E. M. King
43. G. E. Boyd
44. W. J. Ladniak
45. P. R. Bell
46. C. J. Borkowski
47. G. S. Hurst
48. R. S. Livingston
49. E. E. Fairstein
50. C. W. Sheppard
51. W. G. Stone
52. D. D. Cowen
53. C. P. Keim
54. C. D. Susano
55. P. M. Reyling
56. G. C. Williams
57. M. J. Skinner
58-59. J. V. Francis
60. R. W. Johnson
61. D. J. Fisher
62. E. G. Struxness
63. J. R. McNally, Jr.
64. J. L. Gabbard
65. R. A. Charpie
66. T. V. Blosser
67. E. L. Olson
68. J. A. Auxier
69. R. K. Abele
70. J. R. Tallackson
71. H. E. Banta
72. E. W. Burdette
73. R. R. Dickison
74. ORNL Document Reference Library, Y-12 Plant

EXTERNAL DISTRIBUTION

75-76. Ohio State University (Professor of Naval Science)
77. R. Hofstadter, Stanford University
78. J. C. Nance, Consolidated-Vultee Aircraft Corporation
79. J. A. Dever, Minneapolis-Honeywell Regulator Company
80. E. A. Rollor, ANP Project Office, Fort Worth
81. Division of Research and Development, AEC, ORO
82-408. Given distribution as shown in TID-4500 under Instrumentation category

DISTRIBUTION PAGE TO BE REMOVED IF REPORT IS GIVEN PUBLIC DISTRIBUTION

CONTENTS

Investigation of the Response of Scintillation and Cerenkov Counters to the Gamma Radiations from a Swimming-Pool-Type Reactor 1

Differential and Integral Pulse-Height Selector for the DD2 Linear Amplifier 6

An A-C Bridge for Measuring Low Resistances 9

An Improved Serial Memory Pulse-Height Analyzer 11
- Analyzer Performance – Linearity 11
- Resolution Spread and Bias Shift 11
- Stability 11
- Capacity 13
- Future Developments 13

High-Voltage Research 14
- Ion-Source Pulsing System 14

Modifications and Improvements to the Oracle 15
- The Input-Output System 15
- Magnetic-Tape Auxiliary Memory 15
- Cathode-Ray Tube Output Device 15

Instrumentation for Rocking-Bomb Experiments 17

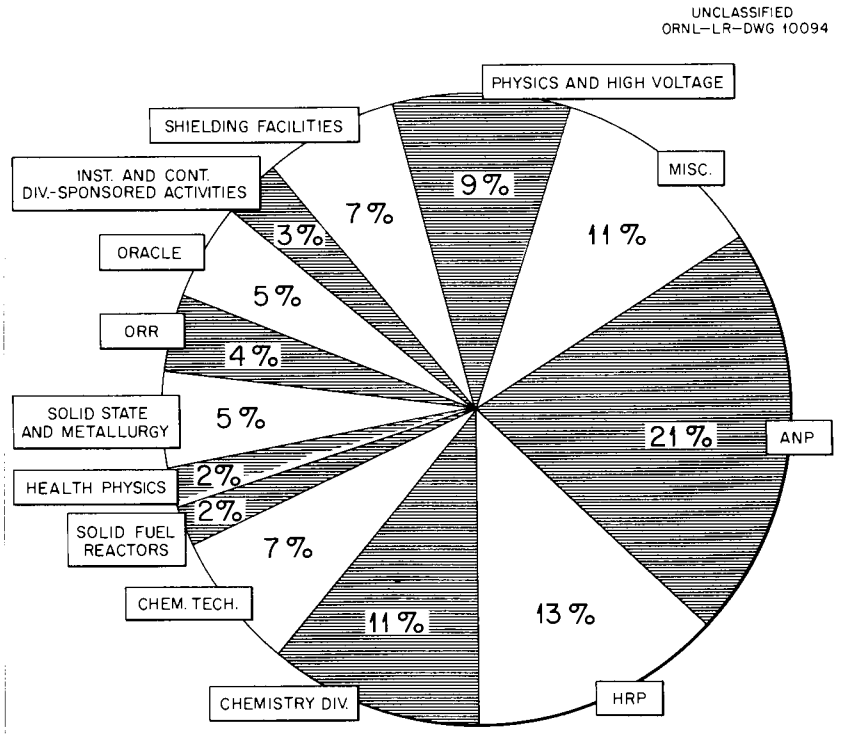

WORK BREAKDOWN OF ENGINEERING AND DEVELOPMENT EFFORTS OF THE INSTRUMENTATION AND CONTROLS DIVISION

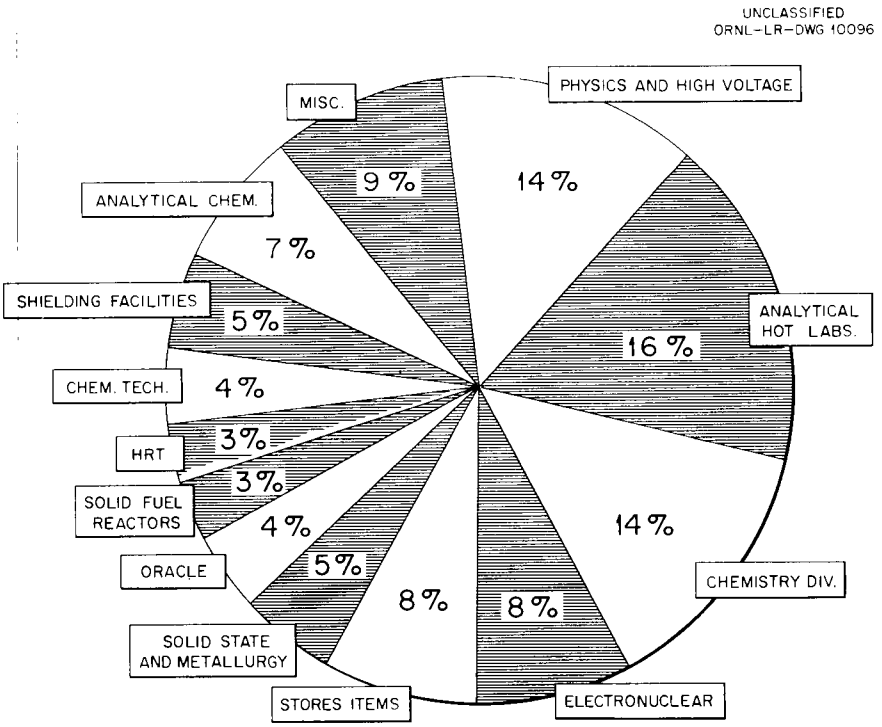

WORK BREAKDOWN OF FABRICATION EFFORTS OF THE INSTRUMENTATION AND CONTROLS DIVISION

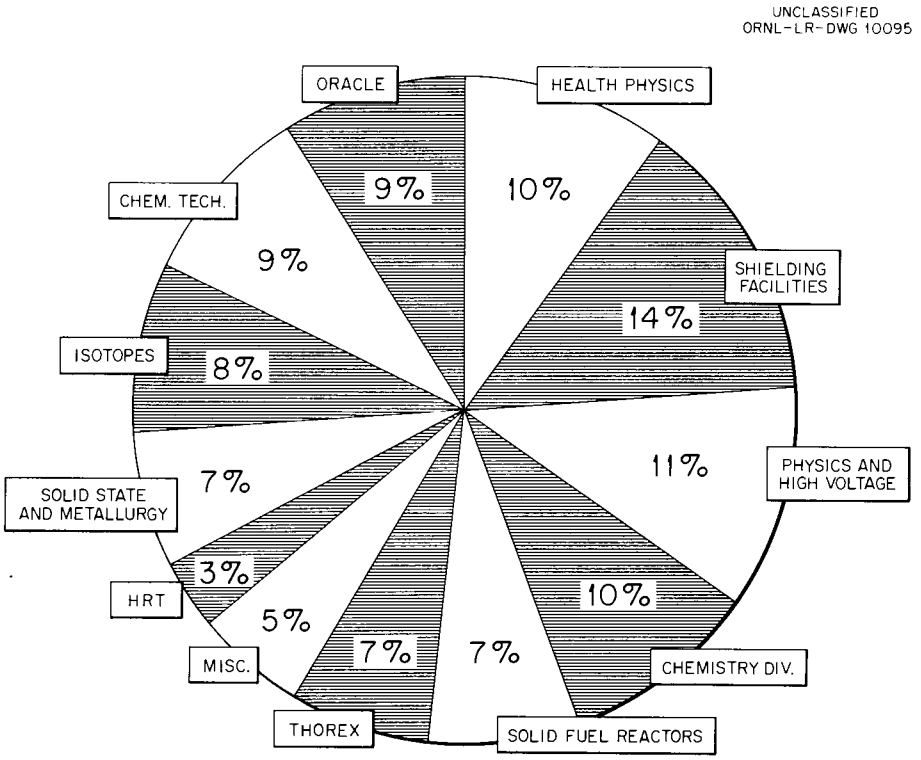

WORK BREAKDOWN OF MAINTENANCE AND INSTALLATION EFFORTS OF THE INSTRUMENTATION AND CONTROLS DIVISION

INSTRUMENTATION AND CONTROLS DIVISION SEMIANNUAL PROGRESS REPORT

INVESTIGATION OF THE RESPONSE OF SCINTILLATION AND CERENKOV COUNTERS TO THE GAMMA RADIATIONS FROM A SWIMMING-POOL-TYPE REACTOR

R. J. Kerr

An experiment has been performed to investigate the response of scintillation and Cerenkov counters to the gamma radiations from a swimming-pool type of reactor and to explore the possibility of using these devices in reactor controls. The gamma-ray spectrum of a swimming-pool reactor shows a considerable flux of energy[1] up to 8 Mev. The energy is composed of prompt-fission gamma rays, neutron-capture gamma rays, and fission-product gamma rays. A gamma-ray detector might be used to indicate reactor power, particularly during startup, by monitoring the gamma-ray flux from the first two of these sources and even that from the fission products if the lifetime of the fission products is less than approximately 10^{-3} sec. Since the radiations from the long-lived fission products are not directly related to the power of the reactor, they should not be counted. Such a gamma-ray detector would have some definite advantages over present neutron-sensitive power indicators in that it would not be greatly affected by the neutron reflectors around the reactor lattice, and in some experimental reactors the detector could be more conveniently located further from the center of the reactor than the location of a neutron detector, since the time required for gamma rays to reach the detector would be much smaller than that for neutrons. In addition, it was of interest to compare this type of detector with the conventional fission chamber.

In the present experiment, scintillators and Cerenkov radiators were used to detect the gamma rays. The scintillators, one a thallium-activated sodium iodide crystal and the other a terphenyl-activated polystyrene phosphor, each measured 3 in. in diameter and 3 in. in thickness. The Cerenkov radiators were distilled water and optical-grade Lucite and were both of the same dimensions as the scintillators. The NaI crystal was packed in MgO, and the other three substances had TiO_2 paint for a reflector. For all measurements, a 3-in. Dumont phototube was optically coupled to the phosphor or Cerenkov radiator. A preamplifier transmitted the electrical pulses from the phototube to a DD2 amplifier.[2] The preamplifier was enclosed, with the phototube and scintillator or radiator, in a watertight housing. An integral discriminator accepted pulses from this amplifier and gave an output to a linear count-rate meter for all those input pulses exceeding its preset bias voltage. Output pulse rate as a function of discriminator bias was recorded at various distances in water from the reactor. With a selected bias voltage, output pulse rate from the discriminator at various reactor power levels was compared with output from a fission chamber and from a compensated ion chamber.

Integral bias curves for the two scintillating substances and both Cerenkov radiators are shown in Figs. 1 through 4. These data were taken in water at 1, 2, and 3 m from the reactor face, with the reactor at approximately 1 w and again with the reactor shut down. Part of the NaI data on the shut-down reactor was taken with "cold" fuel elements (elements not previously in the reactor at power levels above 1 w). These data are represented by the short-dashed lines in Fig. 1. The counting rate at 2 m with the reactor not operating but with "hot" fuel elements was 13.7 times greater than the counting rate from the non-operating reactor with "cold" elements. Data at 1 m on the shut-down reactor with hot elements were not taken. The dot-dash line in Fig. 1 is an assumed value for this spectrum obtained by multiplying the data for cold elements by the factor 13.7. Figure 2 shows integral bias curves for the plastic scintillator, Fig. 3 for the Lucite Cerenkov counter, and Fig. 4 for the H_2O Cerenkov radiator.

[1] F. Maienschein and T. Love, *Nucleonics* **12**, No. 5, 6 (1954).

[2] E. Fairstein, *Instrumentation and Controls Semiann. Prog. Rep. Jan. 31, 1955*, ORNL-1865, p 15.

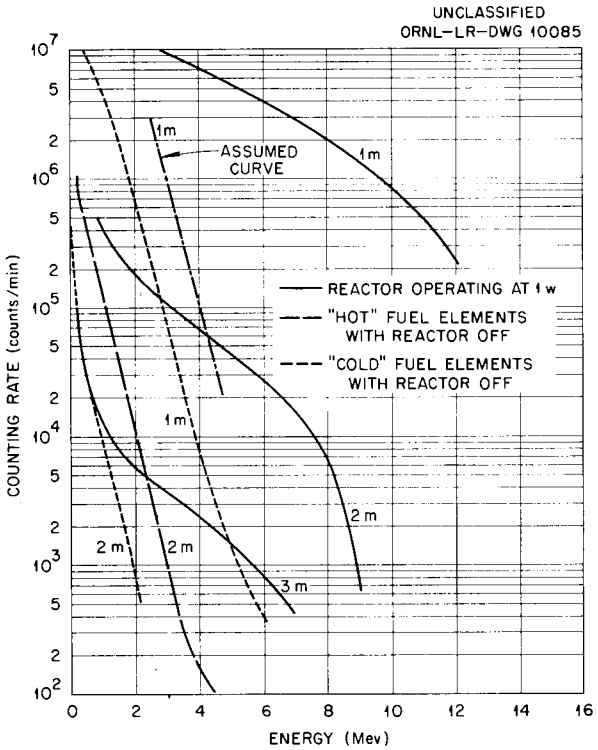

Fig. 1. Integral Bias Curves for NaI(Tl) Scintillator.

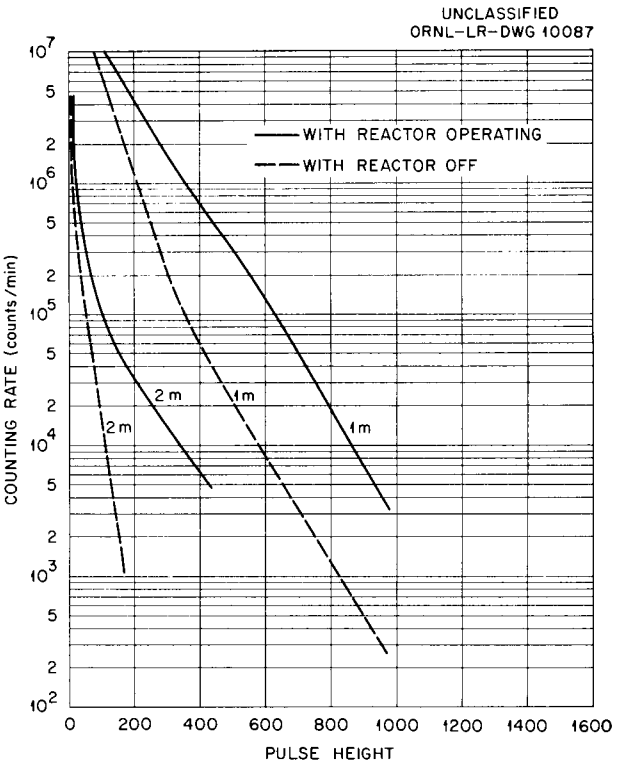

Fig. 3. Integral Bias Curves for Lucite Cerenkov Radiator.

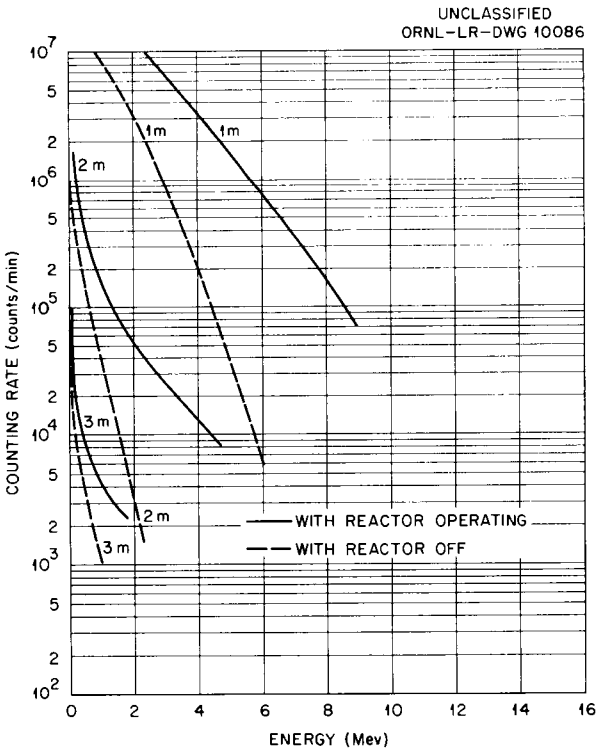

Fig. 2. Integral Bias Curves for Plastic Scintillator.

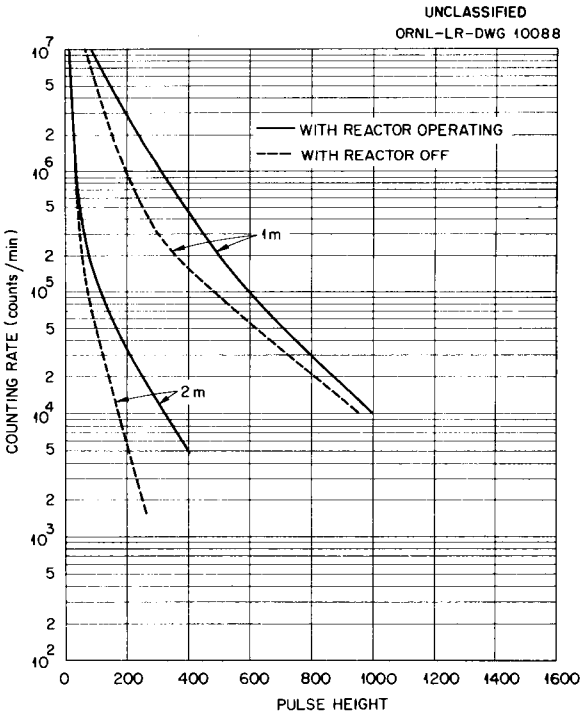

Fig. 4. Integral Bias Curves for Water Cernekov Radiator.

These curves are distorted slightly by random coincidences of pulses at high counting rates. Pulses will pile up in the amplifier if events in the detector are not farther apart in time than the amplifier pulse width. This pileup causes two or more small pulses to be seen by the discriminator as large pulses. Experiments are under way to determine more exactly the effects of pulse pileup at high counting rates with double-delay-line-shaped pulses such as those from the DD2 amplifier. Pileup of square pulses of equal amplitude at random input rates may be calculated.[3] For example, the probability of obtaining any multiple pulse is

$$P = \frac{N_0}{1 + N_0\tau}\left(1 - e^{-N_0\tau}\right),$$

where N_0 is the actual pulse rate into the amplifier, and τ is the pulse width.

If $\tau = 1.2 \times 10^{-6}$ sec and $N_0 = 6 \times 10^6$ counts/min $= 10^5$ counts/sec, then

$$P = \frac{10^5}{1.12}\left(1 - e^{-0.12}\right)$$

$$= (0.893)(0.113) \times 10^5 = 10.1 \times 10^3,$$

and 10.1% of all pulses from the amplifier leave as multiple pulses. Exact calculations are difficult to apply to this actual situation, however, because (1) the pulses have a finite amplitude distribution, (2) they are not exactly square, and (3) they have a negative as well as a positive portion.[2]

The sodium iodide curves (Fig. 1) show the highest ratio of counts with reactor on to counts with reactor off. This is due to the higher efficiency of NaI for stopping gamma rays having higher energies. The ratio of counts from the operating reactor to counts from long-lived fission products (reactor shut down) increases with energy in nearly every case (Figs. 1, 2, 3, and 4): This ratio also increases with distance from the reactor. These two facts suggest that proper choice of discriminator bias and distance in water may be used to minimize the percentage of counts registered from long-lived fission products. Scintillations from the plastic scintillator are emitted about ten times as fast as those from the NaI, so that random coincidences of light pulses in the plastic scintillator are much less probable than in NaI. This did not affect the data taken in this experiment, however, since the probability of pulse pileup was determined by the 2.4-μsec pulse width of the amplifier.

The Cerenkov radiators, given in Figs. 3 and 4, show very low ratios of counts with reactor on to counts with reactor off, indicating their low efficiency for converting gamma rays to fast Compton electrons, which actually are responsible for the Cerenkov light. In order for Cerenkov radiation to be emitted, the velocity of the charged particle must exceed the velocity of light in that medium; that is,

$$v > \frac{C}{u},$$

where

v = velocity of the charged particle,
C = velocity of light,
u = index of refraction of the medium.

Therefore, no electrons below 175 kev in energy were detected in the Lucite (u = 1.5), and none below 260 kev were detected in the water (u = 1.33). This low-energy cutoff in the Cerenkov counters relieves the pulse amplifier somewhat, since there are no pulses from the many electrons present below the cutoff energy. The light output of the NaI scintillator relative to the Lucite Cerenkov radiator was measured with 2.76-Mev gamma rays and with 4.4-Mev gamma rays and was found to be about 500/1.

Figure 5 shows a comparison between counting rate of the NaI scintillation counter biased at 2.8 Mev and readings on the reactor fission chamber and compensated ion chamber, with reactor power varying from approximately 1 to 1/6 w. With the scintillation counter located 2 m from the face of the reactor lattice, and the fission chamber at its nearest point to the lattice, the ratio of scintillation count rate to fission count rate was 1/2.4. (The fission chamber is approximately 6 in. from the top of the active part of the fuel elements at this point.) Fission-chamber counting rate is plotted as the abscissa. As expected, the data points for the ion chamber fall on a straight line passing through the origin. The data points for the scintillation counter also fall in a fairly straight line which crosses above the origin at zero fission count rate. This residual scintillation count rate

[3] B. B. Rossi and H. H. Staub, *Ionization Chambers and Counters*, p 236, McGraw-Hill, New York, 1949.

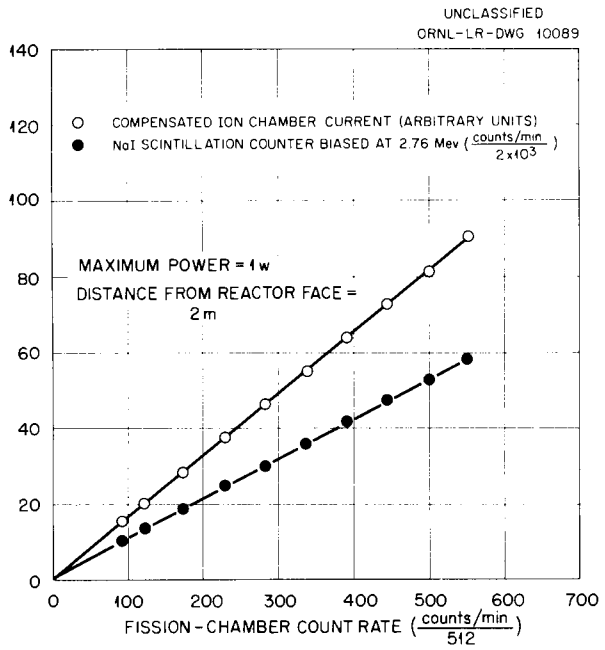

Fig. 5. NaI Scintillator Count Rate as a Function of Reactor Power.

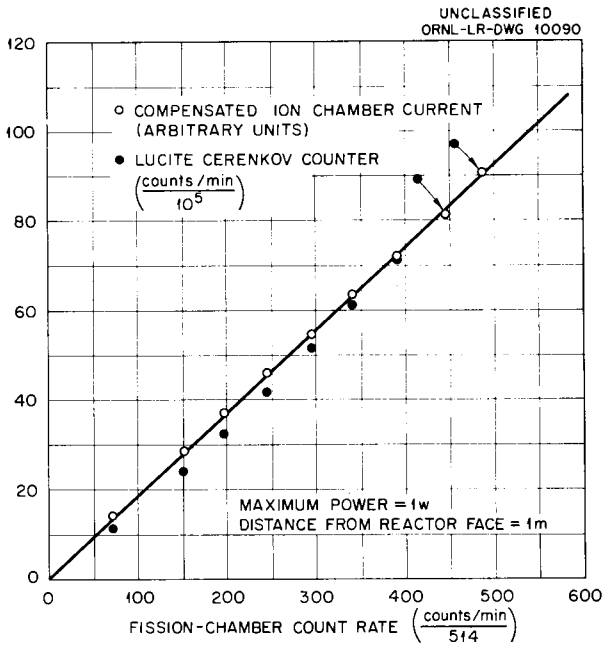

Fig. 6. Counting Rate of Cerenkov Counter as a Function of Reactor Power, at Powers up to 1 w.

is presumably due to pulses from long-lived fission-product gamma rays. At this point these pulses comprise about 1.5% of the total pulse rate.

Figure 6 is a graph of counting rate from the Lucite Cerenkov counter, with the discriminator biased at a point corresponding to 350 pulse-height units on Fig. 3, compared with count rate of the fission chamber. The Cerenkov radiator was 1 m from the reactor lattice, and the fission chamber was at its nearest point to the lattice. The ratio of scintillation count rate to fission count rate is 3.6/1. Readings from the compensated ion chamber are also plotted, and again they fall on a straight line. The data points for the Cerenkov counter curve upward. This may be due to increasing coincidences between pulses from long-lived fission-product gamma rays with increasing reactor power. These coincidences cause pulses to be counted which would normally fall below 350 pulse-height units. The number of long-lived fission-product pulses is large, compared with the number of pulses from the operating reactor, so the total count rate is very sensitive to any changes in long-lived fission-product count rate. Figure 7

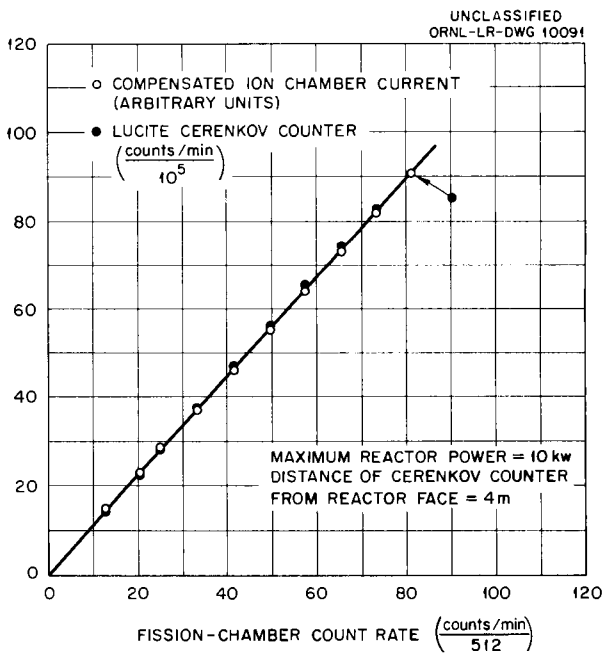

Fig. 7. Counting Rate of Cerenkov Counter as a Function of Reactor Power, at Powers up to 10 kw.

shows Cerenkov counting rate as a function of fission-chamber count rate for reactor powers from 1 w to 10 kw. Ion-chamber readings are again plotted, and they fall on a straight line through the origin, as do the Cerenkov data. This indicates that pileup of low-energy Cerenkov pulses from long-lived fission products was relatively small. Most likely this was because the data were taken through 4 m of water and before long-lived fission products had sufficient time to build up to equilibrium with the 10-kw power level.

These results indicate that biased scintillation counters and Cerenkov counters can be used to indicate reactor power in the low power range by recording the flux of prompt-fission gamma rays and neutron-capture gamma rays and by discriminating against fission-product gamma rays. The NaI scintillator gave the highest ratios of counts from operating reactor to counts from nonoperating reactor. This ratio was approximately 100/1.5 at a distance of 2 m from the reactor face and with the discriminator biased at 2.76 Mev. Under these conditions, the NaI scintillator count rate was 1/2.4 times as great as the fission-chamber count rate, with the fission chamber at its nearest point to the reactor. An interpolation from the data of Fig. 1 indicates that moving the scintillator to 1.7 m from the reactor face would increase its count rate to a value equal to the fission-chamber count rate. This would also make the scintillator counts from the nonoperating reactor equal to 3% of the scintillator counts from the operating reactor at 1 w. The NaI scintillator could, of course, be moved even closer to the reactor lattice to obtain higher counting rates. However, this would raise the percentage of counts from the long-lived fission products and would greatly increase the loading on the amplifier, which must handle all the pulses regardless of the discriminator bias.

The plastic phosphor generally gave lower counting rates and lower ratios of counts from operating reactor to counts from nonoperating reactor. An amplifier with a short pulse length (~ 0.02 μsec) would make use of the faster light emission in this phosphor and should show much greater freedom from pulse pileup.

The Cerenkov radiators used here show comparatively poor ratios of counts from the operating reactor to counts from the nonoperating reactor because of their low stopping power for high-energy gamma rays. Some suitable substance with high density and a high Z should produce better relative response to higher energies. On the other hand, a substance of low density and low index of refraction (~ 1.01) might be used to advantage. Such a radiator would respond only to electrons above about 3 Mev in energy. An integral reading from the photomultiplier could then be taken, and no pulse amplifier or discriminator would be necessary.

DIFFERENTIAL AND INTEGRAL PULSE-HEIGHT SELECTOR FOR THE DD2 LINEAR AMPLIFIER

E. Fairstein

The DD2 linear amplifier[1] is a double-line amplifier designed to operate at counting rates considered to be too high for conventional single-line amplifiers. The single-channel differential pulse-height selector (PHS) circuit designed for use with the A-1 amplifier was modified to make it suitable for operation with the DD2. The circuit is shown in Fig. 8. The operation of the circuit was covered in detail in the report in which it was first described,[2] and it is reviewed here briefly.

In this circuit the signal and bias voltages are applied to the cathode follower, V_1, which is d-c coupled to the four Schmitt trigger tubes, V_2 through V_5. These trigger tubes define the channel edges. The output of the lower trigger circuit is differentiated, thus producing two pips, the second of which is the interrogating signal for the anticoincidence tube, V_7. The output of the upper trigger circuit is stretched by a germanium-diode network to form the inhibiting signal for the second input of the anticoincidence tube. If the input signal operates the lower trigger only, a 24-v, 1-μsec pulse appears at the output terminals. If the input operates both triggers, the anticoincidence circuit prevents the occurrence of an output signal.

The PHS circuit differs from the earlier version in the following significant respects: (1) a cathode follower is provided to drive the trigger tubes, (2) diode restorers are used in all grid circuits where bias shifts would cause improper circuit operation at high count rates, and (3) the 404A tubes initially used in the trigger circuits have been replaced with 403B tubes.

The cathode follower is used to prevent grid current flow (which occurs under overload conditions in the trigger tubes, V_2 and V_4) from causing a bias shift at high count rates. The need for the diode restorers has already been stated.

The use of the Western Electric 403B tubes is a major improvement in this circuit and is made possible by a network that produced the pulse shape shown in Fig. 9. Note that the most positive portion of the pulse occurs about 0.4 μsec before the rapidly falling portion and that the top exhibits a decay of approximately 5%. Triggering action starts at the peak of the pulse, and, with the pulse shape shown, the trigger circuit has about 0.4 μsec in which to come to equilibrium in its quasi-stable state. In earlier circuits, the peak of the pulse occurred at the end, leaving approximately 0.1 μsec for equilibrium to be established. Only tubes with a figure of merit equal to that of the 404A were suitable under these conditions. Type 404A tubes are considerably more expensive than the 403B types and are short lived because of the fact that very close grid-to-cathode spacing is conducive to the development of grid current.

The 403B tubes are electrically interchangeable with 6AK5's and exhibit the additional attributes of having extremely stable cathodes, plus a life expectancy of 10,000 hr. Further, the grid current is no problem in these tubes.

The network for producing the desired pulse shape is shown in Fig. 10. As the circuit indicates, the pulse shaper is placed in the lower section or the third feedback network in the amplifier. This causes a decay whose magnitude can be controlled by the size of C_1 and/or the position of the tap on the lower part of the feedback network. The magnitude of the decay should not exceed the hysteresis of the trigger (about 9 v for the circuit of Fig. 8) at the maximum output of the amplifier or be so small that the peak of the pulse occurs less than 0.25 μsec from the rapidly falling portion. A decay of 5% appears to be optimum. Experience has indicated that variations among amplifiers require that the network be tailored for the particular amplifier in which it is installed.

The DD2 amplifier design included sufficient power capacity and blank chassis space for a spare circuit, making it possible to add the PHS to existing amplifiers.

Performance tests indicate that the slit width is independent of PHS control setting and count rate up to 200,000 cps. The day-to-day drift in the slit width is less than 10 mv. If a 1-v slit is used, this corresponds to a drift of less than 1%. In a two-week test on one of the units, the average drift was zero and the peak drift 10 mv. No measurable drift in the PHS control calibration was observed during this period.

---

[1] E. Fairstein, *Instrumentation and Controls Semiann. Prog. Rep. Jan. 31, 1955*, ORNL-1865, p 15.

[2] E. Fairstein, *Instrument Research and Development Quar. Prog. Rep. Jan. 20, 1951*, ORNL-1021, p 7; also in ORNL-1036, p 65 (Secret).

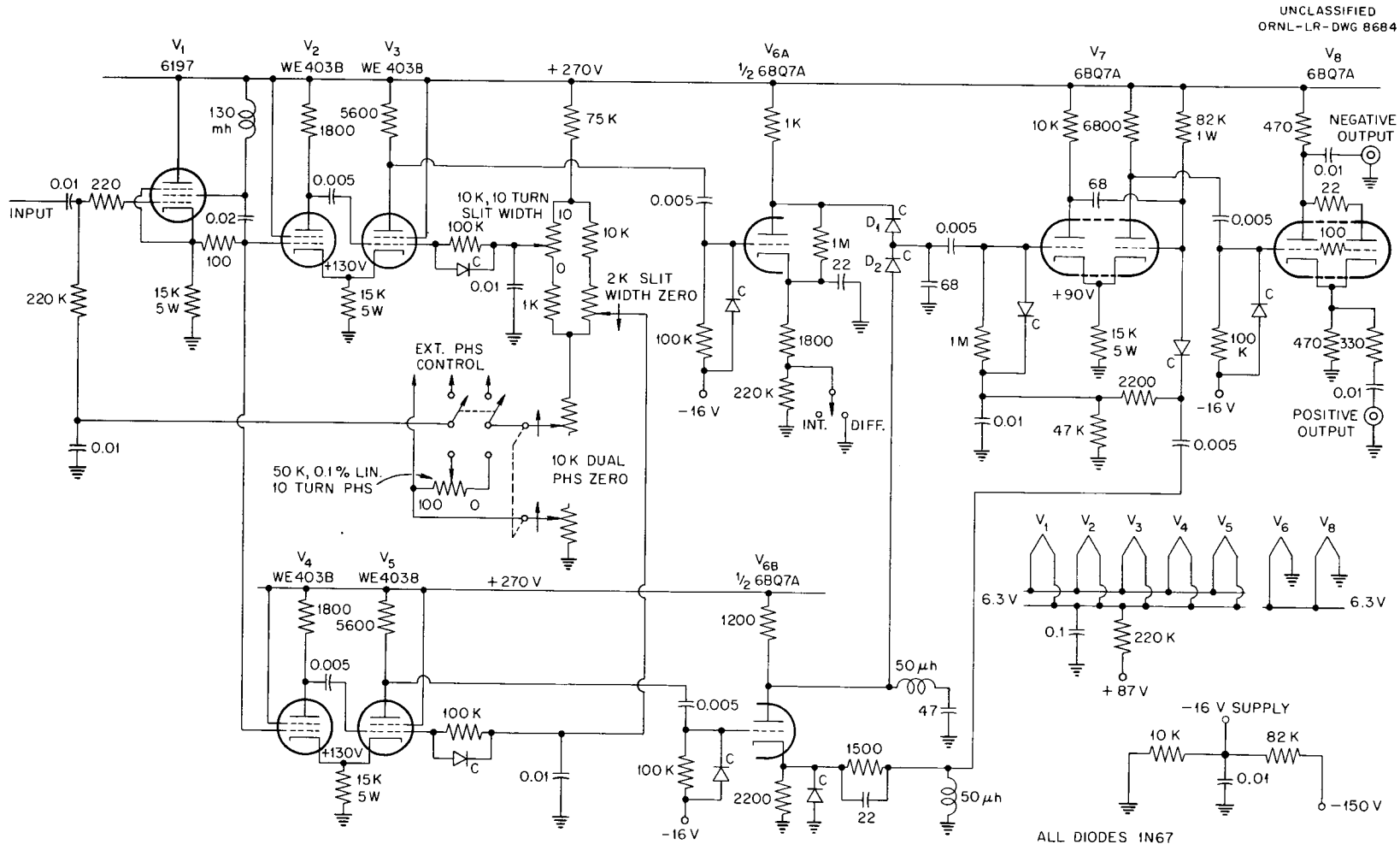

Fig. 8. Circuit Diagram of a Single-Channel Differential and Integral Pulse-Height Selector.

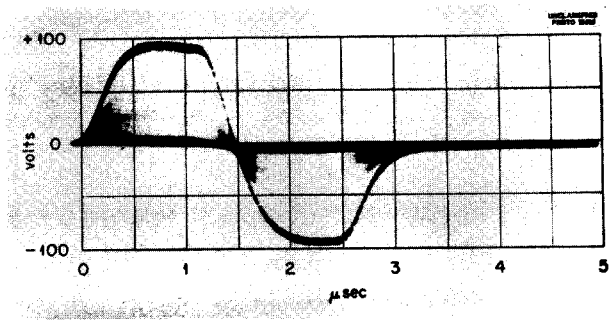

Fig. 9. Amplifier Output Pulse Shape Optimized for Operation of a Pulse-Height Selector.

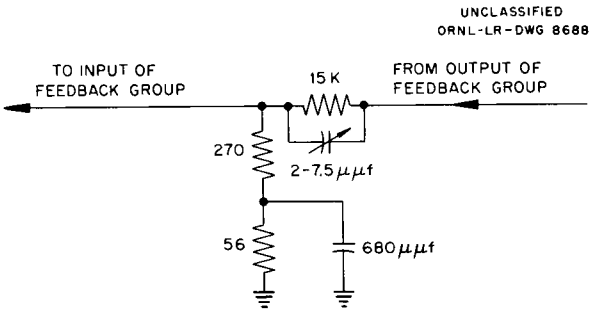

Fig. 10. Feedback Network for Producing a Pulse Whose Top Decays Approximately 5%.

AN A-C BRIDGE FOR MEASURING LOW RESISTANCES

E. Fairstein

At the request of I. S. Yaffe of the Chemistry Division, a resistance bridge was developed that will measure the conductivity of fused salts in the range of 0.01 to 10 ohms.

It was immediately recognized that the use of a four-terminal conductivity cell would be mandatory because of the difficulty of correcting for connecting-lead resistance, reactance, and the polarizing effect of the electrode-liquid interface. The cell configuration adopted is shown in Fig. 11. The concentric rings are made of platinum, and the support wires are made of a platinum-rhodium alloy. The liquid level is maintained just above the top edges of the rings.

The use of a bridge-type measurement was selected because of its simplicity of operation, accuracy, and the relatively low cost of the essential components. The four-terminal cell and standard are converted to two-terminal networks by transformers.

The basic bridge circuit is shown in Fig. 12. The operating range is 200 to 6000 cps. The power source is capable of supplying 1 amp to R_s and R_x, the standard and the unknown, respectively; R_s is adjustable from 0.1 to 5.0 ohms. The residual polarization of the cell, which is represented by the capacitor C_x, and the unavoidable mutual inductance of the current and potential leads in the cell are resonated by the adjustable mutual inductance, M. A maximum inductance of approximately 10 μh proved sufficient for this purpose. The resistances R_1 and R_2 are 12,000-ohm decade boxes, and C_1 and C_2 are 200-$\mu\mu$f variable capacitors which permit the equalization of the time constants R_1C_1 and R_2C_2. The null detector consists of a low-noise preamplifier of conventional design followed by an oscilloscope; the preamplifier has a gain of 25,000. The ultimate sensitivity is obtained when the x and y deflection amplifiers are connected to the bridge supply oscillator and preamplifier, respectively, to give a Lissajou figure on the screen. A Wagner ground is also provided to balance the effect of primary-to-secondary capacitance in the transformers; its adjustment is noncritical.

The use of a bridge as a measuring instrument in this application would have been quite impractical, if not impossible, were it not for the transformers. Even through their use, the bridge is practical over a 10:1 frequency range only if the transformers have closely matched turns ratios and extremely wide frequency ranges. The transformer type chosen was the General Radio 941. This model is toroidally wound and has four separate windings which can be connected in various combinations to provide a number of different turns ratios. A ratio of 1:1 proved satisfactory, and the approximate equivalent circuit is shown in Fig. 13.

UNCLASSIFIED
ORNL-LR-DWG 6977

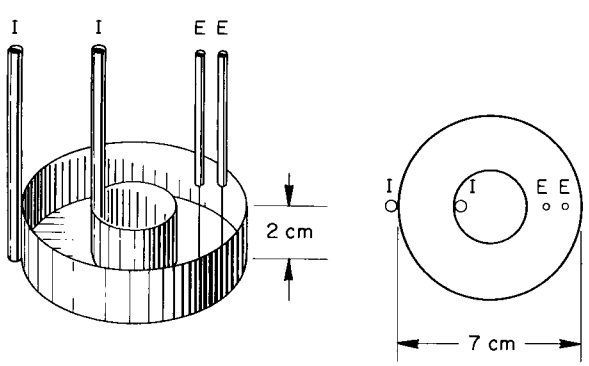

Fig. 11. Fused-Salt Conductivity Cell.

UNCLASSIFIED
ORNL-LR-DWG 6978

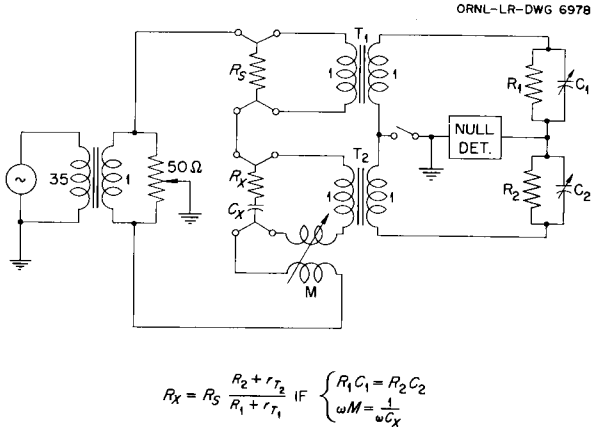

Fig. 12. Fused-Salt Conductivity Bridge.

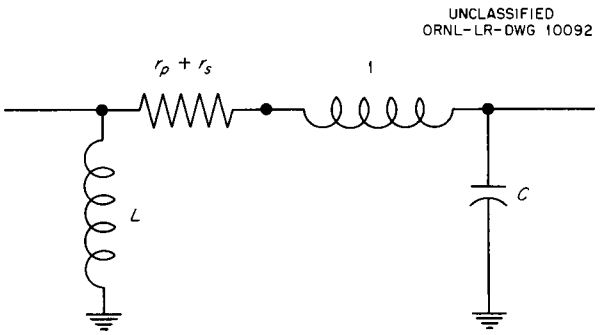

Fig. 13. Transformer Equivalent Circuit.

The primary inductance is at least 10 h and has a reactance of approximately 10,000 ohms at 200 cps, the lowest operating frequency of the bridge. The primary-winding resistance is approximately 8 ohms. If the maximum resistance across which the transformer is connected is 10 ohms, the effect of the primary inductance is to attentuate the signal by approximately 0.1%. Raising the operating frequency to 600 cps, or reducing the resistance to 3 ohms, decreases the correction 0.01%.

The leakage inductance, L, is approximately 500 μh, and the shunt capacitance, C, is about 400 $\mu\mu$f. At 6 kc, the signal level is increased by 0.015%. The primary and secondary resistances, r_p and r_s, amount to about 18 ohms and must be added, at the balance point, to the resistances R_1 and R_2 shown in Fig. 12.

To summarize, the effective equivalent circuit for the transformer is that of a pure resistance of about 18 ohms which must be added to the arm of the bridge to which the transformer is connected. The error introduced by this approximation is less than 0.02% if the operating frequency is within the 500- to 6000-cps band. Also, it appears that the turns ratios match to approximately 0.02% in these transformers, at least for the four that were tested.

In using the bridge, a preliminary null is obtained with the switch (shown in Fig. 12) in the closed position. The switch is then opened, thus floating the transformer secondaries. The 50-ohm Wagner ground is then adjusted for null, the switch is closed again, and the bridge is rebalanced. If the transformers contained electrostatic shields between primary and secondary, the Wagner ground would not be necessary.

At balance, the unknown resistance may be found from the equation

$$R_x = R_s\left(\frac{R_2 + r_{T_1}}{R_1 + r_{T_2}}\right)\left[\frac{1 + 4^2f^2R_1C_1R_2C_2}{1 + 4^2f^2(R_2C_2)^2}\right],$$

where r_T is the equivalent series resistance of the transformer, and f is the operating frequency. If the condition $R_1C_1 = R_2C_2$ or $C_2 = 0$ can be met, the equation is reduced to

$$R_x = R_s\left(\frac{R_2 + r_{T_1}}{R_1 + r_{T_2}}\right);$$

C_2 can never be made zero, since it includes the parasitic capacitance of the decade box. However, it can be kept down to approximately 30 $\mu\mu$f. If R_2 = 10,000 ohms and f = 6 kc, the denominator of the correction term becomes approximately 1.0001. The correct value of R_1C_1 which would give the same numerator is identical to the value of R_2C_2, as stated above. If it is higher by a factor of 3, the numerator becomes 1.0003, leading to a net correction of only 0.02%.

It is evident from the above example that, even at a frequency of 6 kc, good accuracy can still be obtained if the correction term introduced by improper setting of the C_1 and C_2 dials is ignored.

In a test of the bridge in which high-quality a-c standard resistors were used and where corrections were made for errors in the decade boxes, it was possible to measure the value of a resistor of 0.1 ohm in terms of a second standard of 0.5 ohm to an accuracy of 0.03%, which was the rated accuracy of these resistors. This value remained unchanged in the range from 300 to 5000 cps. The sensitivity of balance was 0.002%.

It is felt that this circuit is capable of yielding accuracies of better than 0.01% if sufficiently good components are obtained. The accuracy of conductivity-cell measurements is not so good as the bridge accuracy. This is probably because of polarization effects in the cell. I. S. Yaffe will discuss this problem in a separate report.

R. A. Dandl and F. M. Porter have contributed materially to the success of this instrument by their helpful suggestions during its development.

AN IMPROVED SERIAL MEMORY PULSE-HEIGHT ANALYZER

T. L. Emmer

In the design of a pulse-height analyzer, for a given accuracy and stability, the cost of the analyzer must be balanced against analyzing speed. Generally, the storage system of the analyzer will determine both the cost and analyzing speed, since fast analyzers have more expensive parallel memory storage systems, as compared with the cheaper serial memory storage systems of slower analyzers. By using an acoustical delay line in a serial memory analyzer, it is possible to obtain an accurate, stable analyzer with a large storage capacity at a reasonable cost.

The first multichannel pulse-height analyzer using a mercury acoustical delay-line memory was designed and constructed by Hutchinson and Scarrott at Cambridge University.[1,2,3] A 100-channel analyzer of this type was built and has been operating at ORNL for the past year and a half.[4,5] By using the experience gained in the construction and operation of this analyzer, a 120-channel analyzer (shown in Fig. 14) was constructed which incorporated modifications for improving the resolution, linearity, stability, and capacity.

In most pulse-height-to-time analyzers, a pulse to be analyzed is commonly lengthened and compared with a linear sweep. When the pulse voltage and linear-sweep voltage are equal, a count is placed in the memory. Information is stored in the memory of this type of analyzer as sequences of pulses which are continually recirculated through an acoustical delay line. The information in the memory is then monitored by a cathode-ray tube display. Figure 15 shows a photograph of the display for the gamma-ray spectra of Y^{88}, Cs^{137}, Be^{7}, and Hg^{203}. The sources were analyzed in the order of decreasing energy, with the lower-level discriminator set above the Compton distribution in each case, except for Hg^{203}. Each vertical row of dots represents a channel in the pulse-height spectrum, and the order of dots in each channel represents the number of pulses counted in that channel in binary notation; that is, a dot in the lowest position is 2^0 counts, one in the second position is 2^1 counts, etc. The total count in each channel is then the vertical sum of the dot representation.

Analyzer Performance – Linearity

A plot of the spectrum of Fig. 15 is shown in Fig. 16. By plotting the binary numbers on binary log paper, the spectrum can be plotted quickly to an accuracy of 3% by using only the top five binary numbers in each channel. For this experiment the analyzer was adjusted so that the channel number corresponded to the energy in Mev/100. The correlation of energy vs channel number was such that each peak fell into the correct channel within less than a channel width, corresponding to a linearity of about ±1%. This figure has been checked with a precision pulse generator.

Resolution Spread and Bias Shift

In order to check the resolution spread and bias shift at varying counting rates, pulses from a pulse generator were mixed with the output of a scintillation spectrometer at the input of the preamplifier. The pulse-generator pulses were analyzed in the presence of a varying background obtained by placing Co^{60} sources of increasing intensities on the detector. Figure 17 shows the curves-of-resolution spread and bias shift vs input counting rate observed in the above experiment.

Stability

For this type of analyzer, interchannel drift should be virtually eliminated, since one discriminator is used for all channels. By using a system of blocking-oscillator dividers driven by the binary-bit clock signal for setting the channel boundaries, it was possible to obtain better channel

[1] G. W. Hutchinson and G. G. Scarrott, *Phil. Mag.* **42**, 792 (1951).

[2] A. B. Van Rennes, *Nucleonics* **10**, No. 10, 50, esp. 53–55 (1952).

[3] G. W. Hutchinson, *Nucleonics* **11**, No. 2, 24 (1953).

[4] T. L. Emmer and R. D. Sidnam, *Instrumentation and Controls Semiann. Prog. Rep. July 31, 1954*, ORNL-1768, p 7.

[5] T. L. Emmer, "Serial Memory 100-Channel Pulse Height Analyzer," 1955 IRE Convention Record, vol 3, part 10, p 211–217.

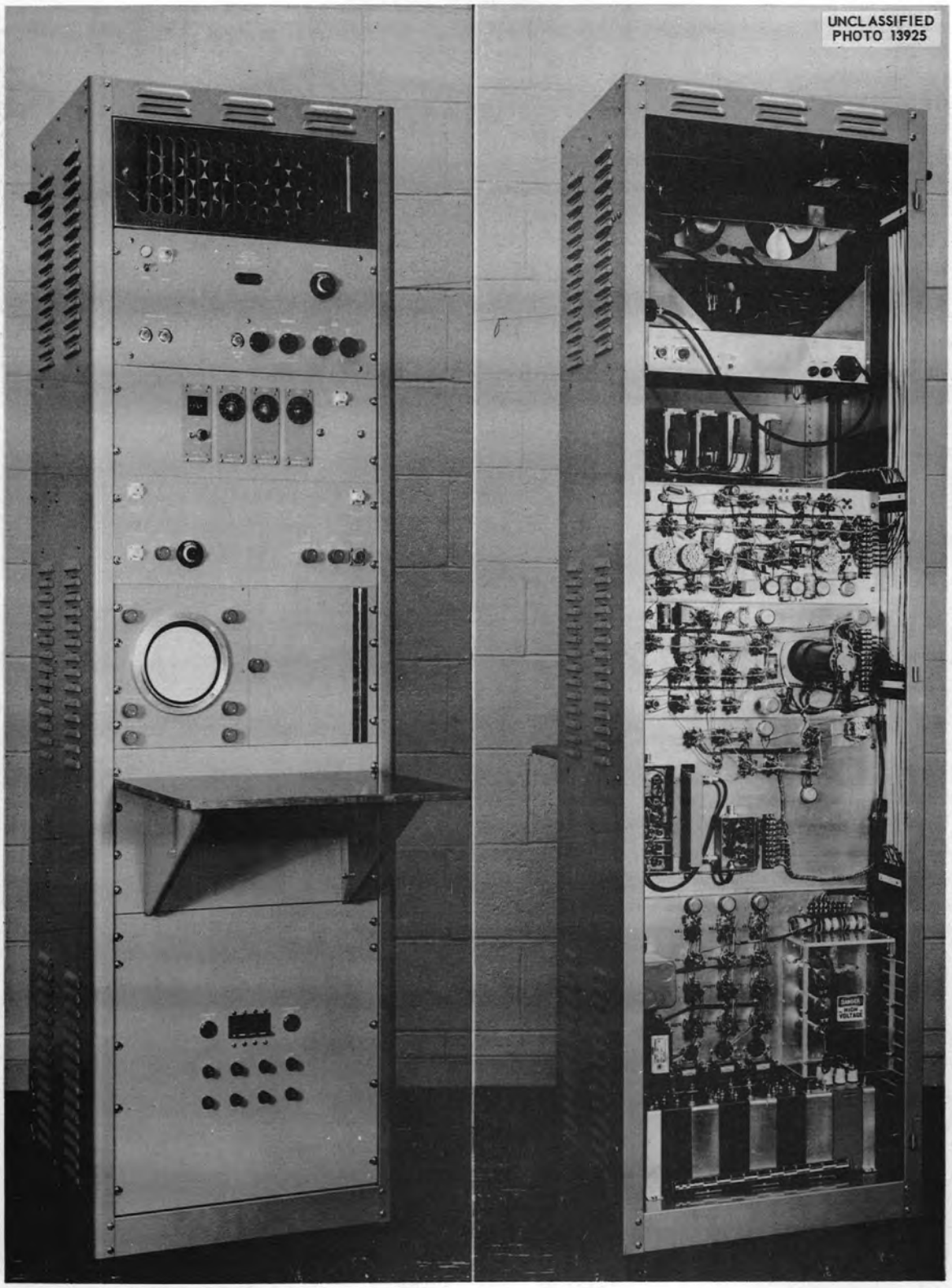

Fig. 14. Serial Memory 120-Channel Pulse-Height Analyzer.

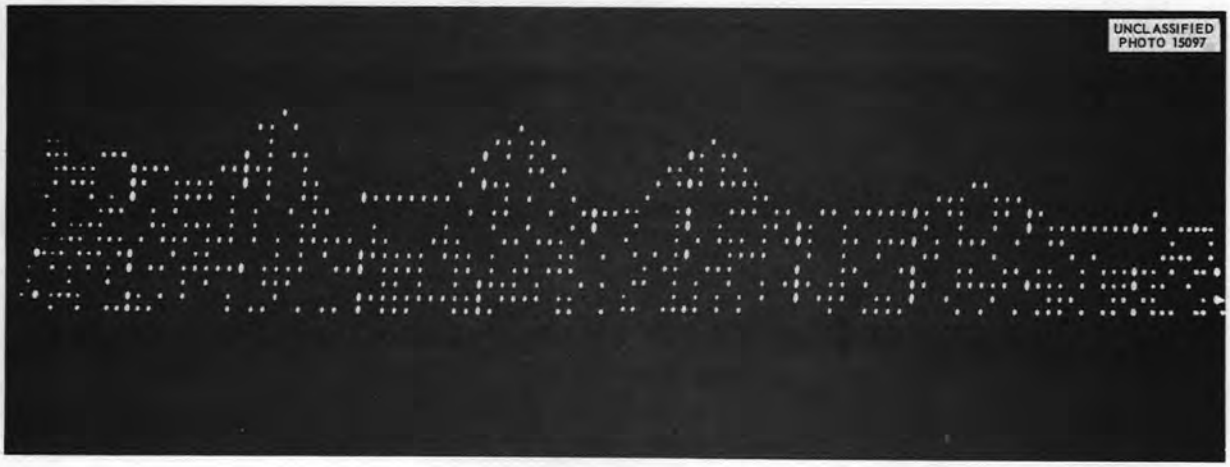

Fig. 15. Cathode-Ray Tube Display for Some Gamma-Ray Spectra.

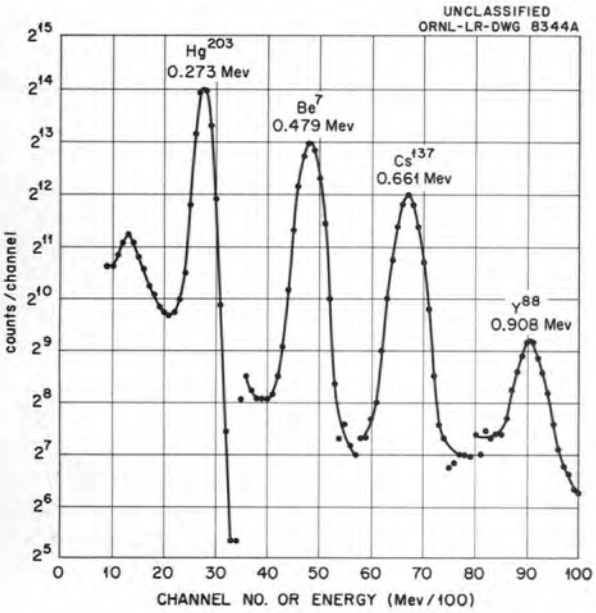

Fig. 16. Binary Log Plot of Cathode-Ray Tube Display.

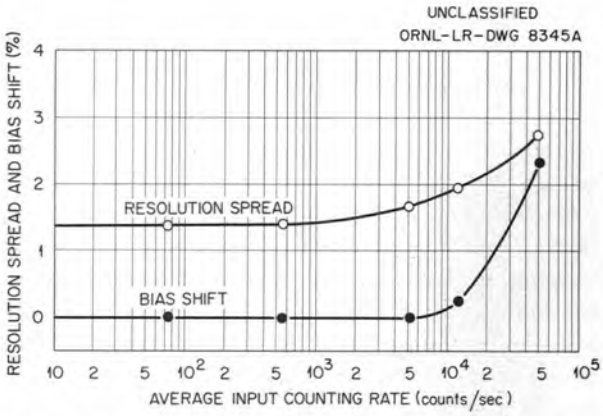

Fig. 17. Resolution and Bias Shift vs Input Count Rate.

stability than by the previous system wherein a channel oscillator was synchronized with the clock. With this technique and careful regulation of the power supplies, it was possible to keep the over-all drift to less than 1% for periods of a day.

Capacity

Since quartz delay lines can be designed to have wider bandwidths than mercury delay lines, a 1000-μsec quartz delay line was chosen for the memory of the 120-channel analyzer. It was then possible to increase the packing rate into the delay line, thus increasing the storage capacity from 5000 counts/channel for 100 channels to 65,000 counts/channel for 120 channels.

Future Developments

Work is being done at the present time on a print-out system for the 120-channel analyzer. This printer will transcribe the binary count in each of the 120 channels to decimal form and print at a rate of about 1 sec per channel.

HIGH-VOLTAGE RESEARCH

H. E. Banta R. F. King
V. E. Parker[1]

The 625-kv cascade generator has been placed in operation. In this installation, the generator, a G-E unit, operates on the third floor of the building, and the high voltage is passed through the floor, by means of a vacuum bushing, to the accelerator tube on the level below. The bushing, which is approximately 20 ft in length and weighs approximately 1200 lb, has given some trouble from the standpoint of voltage breakdown but is now in operation and is working satisfactorily in a residual argon pressure of 5×10^{-4} mm.

Ion-Source Pulsing System

An ion-source beam pulser has been developed for use in neutron time-of-flight experiments. It has been installed on the cascade accelerator for a test run and has delivered bursts of ions 16 mμsec in duration at a repetition rate of 10^6 per second and a peak current of 200 μa.

Neutron time-of-flight work currently in progress at the Laboratory makes use of a beam deflector or chopper to interrupt the accelerated beam and is limited by accelerator tube loading and by the neutron background produced when the deflected beam is off the target. By pulsing the beam before it enters the accelerator, both of these limitations can be reduced.

A beam pulser consisting of a lens and a set of beam deflector plates was designed to fit between the ion source and an aperture placed at the entrance to the accelerator tube. The function of the lens was to bring the ion beam to focus at the aperture. Radio-frequency voltage up to 4000 v rms at 500 kc was applied to the deflector plates to sweep the focused beam across the aperture. The beam passed through the aperture and entered the accelerator tube for only a short interval of time near the zero axis of the sweep voltage.

After test-bench experiments, the pulser was installed on the 625-kv cascade accelerator, with a fixed aperture 150 mils in diameter. As on the test bench, the best method of tuning was to set a desired value of extraction voltage and coil current, then adjust the accelerator lens voltage, the unipotential lens voltage, and the sweep voltage for the most uniform pulse height and desired length, as displayed on a Tektronix model 517 oscilloscope. All three of these adjustments interacted, somewhat, with each other. The focused but unswept proton beam on the target had a current of 150 to 200 μa, appeared to be circular in cross section, and was well-focused to a diameter of 100 mils. Upon turning on the sweep voltage, the 100-mil spot would change to a line 100 mils wide and $\frac{3}{4}$ in. long.

The duration of these short pulses could not be accurately measured with the oscilloscope. The time spread of the gamma rays produced by bombarding a lithium target with the pulsed proton beam at an energy of 500 kev was measured by a multichannel time analyzer built by J. H. Neiler and known to have a resolving time of less than 7 mμsec. Pulses were produced that had steep sides, quite short tails, and were 16 mμsec wide at half maximum. The average current on the target was about 1.5 μa or approximately 1% of the unpulsed beam current.

It is planned to install the beam pulser in the 2.5-Mv Van de Graaff in the near future, and a radio-frequency oscillator and power supply are now being designed to fit in this restricted space.

[1]Research participant, Louisiana State University.

MODIFICATIONS AND IMPROVEMENTS TO THE ORACLE

W. J. Gerhard J. W. Woody
R. J. Klein

The Input-Output System

The design of a completely new input-output system to improve the flexibility, speed, and reliability of the Oracle has been undertaken. This system will improve (1) the flexibility, by allowing alphabetic characters and special symbols to be used in the computer in addition to the number characters already available; (2) the machine speed, by increasing the output speed by a factor of 50; and (3) the reliability, by using a parity checking system to ensure the correct transfer of information through all tape-handling equipment as well as through all input and output equipment.

Paper tape will be used as an input medium, while paper tape, magnetic tape, and printed pages will be used for output media. Auxiliary equipment to accommodate both paper and magnetic tapes will allow four times as much tape processing and printing to be accomplished as is now possible. By the use of editing routines in the computer, it will be possible to produce the results of computations in neat tabular form (see block diagram, Fig. 18).

Magnetic-Tape Auxiliary Memory

Installation and trouble-shooting on the large-capacity magnetic-tape auxiliary memory unit for the Oracle are nearing completion. Only the tape-supply reel-sensing devices remain to be installed. Considerable effort has been expended in obtaining a suitable type of magnetic tape in sufficient quantity for use with this device. This is primarily because tape width and coating uniformity must be controlled. The problem is currently being discussed with several tape manufacturers in an effort to obtain a more desirable product.

Although this auxiliary memory has been in operation for only a short time, several large problems have already made successful use of its vast storage capacity, which is of the order of 4,000,000 Oracle words. It is anticipated that this capacity will be doubled on or about October 10, 1955.

Cathode-Ray Tube Output Device

A cathode-ray tube curve plotter for the Oracle is under construction at the present time. This equipment will contain the following components:

1. an electrostatically deflected and focused cathode-ray plotting tube,
2. a digital-to-analog converter for allowing the computer to control the deflection of the electron beam in the plotting tube,
3. an automatic camera for making permanent records of the plot,
4. a monitor tube for allowing constant visual inspection during the plotting operation.

The plotting speed will be of the order of 200 μsec per point, thus permitting extremely rapid data output in graph form which, for most problems, will be easier to analyze than numerical information. Special facilities are also being considered for allowing this device to produce very rapid digital output from the Oracle.

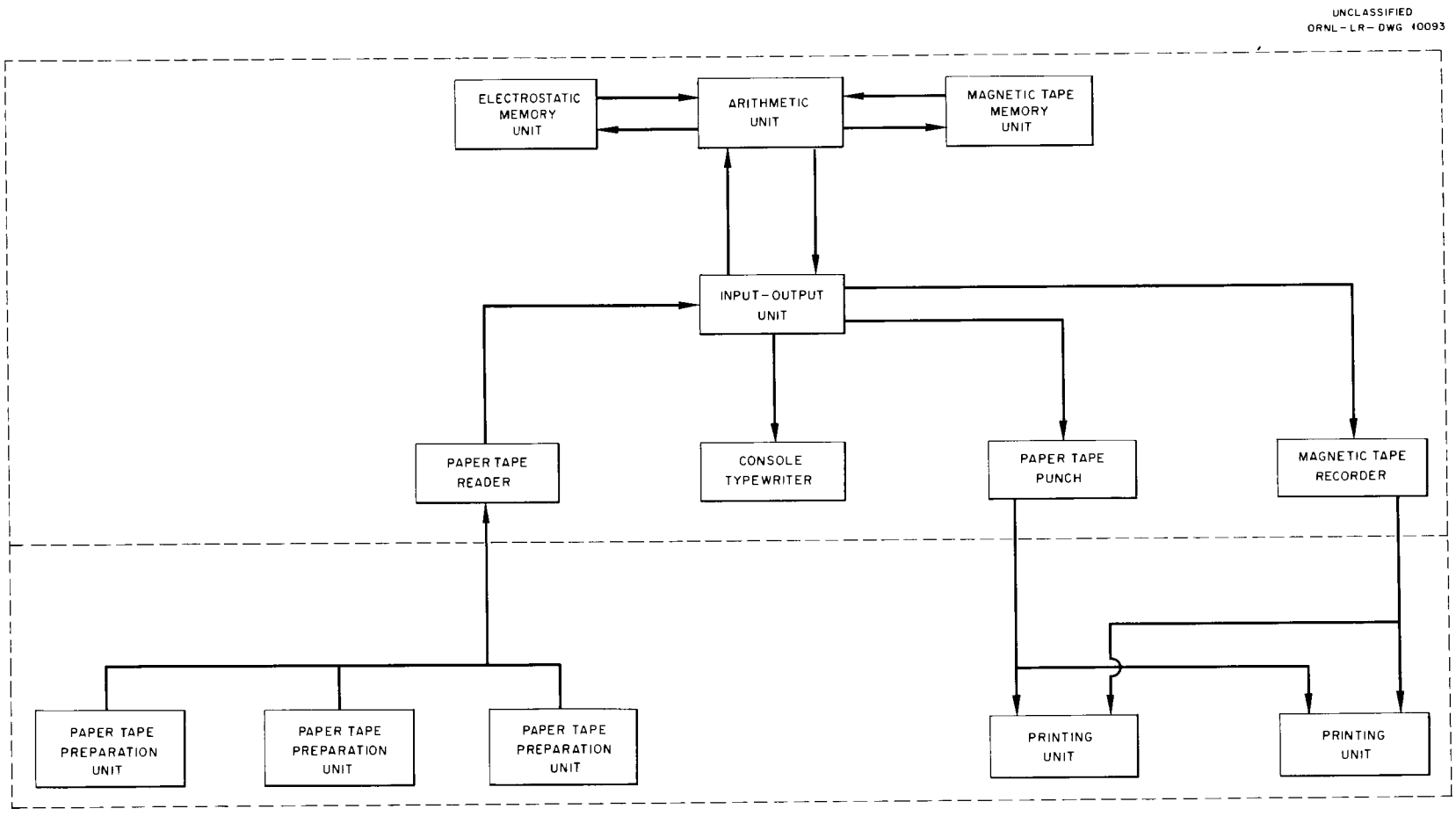

Fig. 18. Oracle Auxiliary Equipment Block Diagram.

INSTRUMENTATION FOR ROCKING-BOMB EXPERIMENTS

G. Ritscher

The rocking-bomb experiments consist of a series of tests in the MTR by the Chemistry Division to determine the effects of high-level radiation on solutions. The instrumentation requirements include the following:

1. bomb temperature control,
2. bomb temperature and pressure recording,
3. provisions for retracting experiments from reactor flux,
4. radioactivity monitoring,
5. power-reduction signals in the reactor,
6. provision for a central control and alarm panel.

Temperatures are measured by using thermocouples with conventional potentiometer and millivoltmeter circuits. An innovation to this is the use of an automatic thermocouple switchover circuit which provides, in the event of failure of the first thermocouple or a high-temperature indication, for a measurement by a second thermocouple before signals are sent to the reactor for reduction of power. Pressure is read with a Baldwin pressure cell and a potentiometer that has been modified to standardize against the voltage of the pressure-cell circuit. This allows operation without manual adjustments.

The installation of the instrumentation has been completed, and the system has performed satisfactorily.